Nonlinear Dyn (2019) 97:123–134
https://doi.org/10.1007/s11071-019-04958-y

ORIGINAL PAPER

Continuation of periodic solutions of various types of delay differential equations using asymptotic numerical method and harmonic balance method

Louis Guillot · **Christophe Vergez** · **Bruno Cochelin**

Received: 22 November 2018 / Accepted: 15 April 2019 / Published online: 27 April 2019

Abstract This article presents an extension of the asymptotic numerical method combined with the harmonic balance method to the continuation of periodic orbits of delay differential equations. The equations can be forced or autonomous and possibly of neutral type. The approach developed in this paper requires the system of equations to be written in a quadratic formalism which is detailed. The method is applied to various systems, from Van der Pol and Duffing oscillators to toy models of clarinet and saxophone. The harmonic balance method is ascertained from a comparison to standards time-integration solvers. Bifurcation diagrams are drawn which are sometimes intricate, showing the robustness of this method.

Keywords Nonlinear dynamics · Delay equations · Harmonic balance method · Numerical continuation · Periodic solutions · Quadratic recast · Asymptotic numerical method

L. Guillot (✉)· C. Vergez · B. Cochelin
Aix Marseille Univ, CNRS, Centrale Marseille, Laboratoire de Mécanique et d'Acoustique UMR 7031, 4 impasse Nikola Tesla, 13013 Marseille, France
e-mail: guillot@lma.cnrs-mrs.fr

C. Vergez
e-mail: vergez@lma.cnrs-mrs.fr

B. Cochelin
e-mail: bruno.cochelin@centrale-marseille.fr

1 Introduction

The aim of this article is to extend the framework of the numerical continuation of periodic solutions of differential systems using the harmonic balance method (HBM) coupled with the asymptotic numerical method (ANM) to time-delay systems.

The HBM, a frequency-based method to search for periodic solutions of dynamical systems, has its roots in Fourier theory [13]. The works [20,22] developed the HBM as we know it today. Its application to delay differential equations (DDE) has been done in [21], using an alternating frequency–time scheme. The originality of our work is that all the steps of resolution are treated directly in the frequency domain without any incursion in the time domain and thus without possible aliasing errors. From this point of view, the order of truncation of the Fourier series is the only source of error.

The ANM, a Taylor series-based continuation method, was first introduced in [4,5] for the computation of equilibrium of nonlinear structures [30]. This is an alternative to more common predictor–corrector methods [23], and it can be seen as a high-order predictor that does not need any correction step. A few developments based on this method are given below.

For dynamical systems without delay, the efficiency of the ANM coupled with the HBM has already been shown in several works (see [8,18] and [27] for some examples). The work [16] treats the case of quasi–periodic solutions using the same framework. To achieve better efficiency, the choice to recast the origi-

nal system into a quadratic version has been done. The procedure to obtain such a recast has been explained in great detail in [15] and is briefly recalled in this paper. The way to recast non-polynomial nonlinearities was explained for the first time in [18], and a way to recast fractional order derivatives is already known from [28]. As opposed to already existing methods of continuation of delay differential equations (DDE) (see [12] and its adaptation for neutral systems [2]), the method developed in this paper is based on the frequency representation of the periodic solutions. For smooth systems, this often is an advantage as the convergence properties of the frequency representation (the Fourier series) are very good. In addition, the robustness of the ANM will be shown to overcome some inherent difficulties of DDE.

This article contains three sections. In the first section, the ANM and the HBM are recalled. It is admitted that the method can be applied to virtually any explicit or implicit differential-algebraic equations. It is extended in a second section to the case of explicit or implicit delay algebraic-differential equations which can be forced or autonomous. Neutral systems can also be treated. The effect of time delay on Fourier series is derived, and the use of auxiliary variables to write the delayed variable in the frequency domain is detailed. This makes the quadratic recast of a delayed variable clear. In the last section, the method is applied to several examples, showing its versatility and its robustness particularly when applied to neutral systems. The convergence of the Fourier series with the order of truncation is shown, and the solutions are compared to standard time-integration solvers. The continuation with respect to the delay is also explored in the first example.

2 Continuation of periodic solutions

2.1 Harmonic balance method

As described in [8], the periodic solutions $t \mapsto x(t)$ of a dynamical systems are represented by their truncated Fourier decomposition which is found through the harmonic balance method:

$$\begin{aligned} x(t) &= \sum_{k=-H}^{H} x_k \exp(ik\omega t) \\ &= a_0 + \sum_{k=1}^{H} a_k \cos(k\omega t) + b_k \sin(k\omega t) \end{aligned} \tag{1}$$

where ω is the pulsation of the oscillations and H is the number of harmonics, i.e. the order of truncation of the Fourier series. Given that x_{-k} is the complex conjugate of x_k, the complex form and the real form of the Fourier series are equivalent; hence, both can be used depending on which is more convenient.

For example, let us seek periodic solutions of

$$\ddot{x} + 2\mu\dot{x} + x + x^3 = F\cos(\omega t) \tag{2}$$

The system is rewritten quadratically as in [8] :

$$\begin{aligned} \ddot{x} + 2\mu\dot{x} + x + xy &= F\cos(\omega t) \\ y &= x^2 \end{aligned} \tag{3}$$

The next step is to compute products and derivatives directly on the complex form of Fourier series (1). The products can be written as a convolution :

$$\begin{aligned} &\left(\sum_{k=-H}^{H} x_k \mathrm{e}^{ik\omega t}\right)\left(\sum_{k=-H}^{H} y_k \mathrm{e}^{ik\omega t}\right) \\ &= \sum_{k=-H}^{H} \mathrm{e}^{ik\omega t} \sum_{\substack{h_1+h_2=k \\ |h_1|\le H, |h_2|\le H}} x_{h_1} y_{h_2} \end{aligned} \tag{4}$$

The derivatives can be written :

$$\begin{aligned} \dot{x}(t) &= \textstyle\sum_{k=-H}^{H} ik\omega x_k \mathrm{e}^{ik\omega t} \\ \ddot{x}(t) &= \textstyle\sum_{k=-H}^{H} -k^2\omega^2 x_k \mathrm{e}^{ik\omega t} \end{aligned} \tag{5}$$

Now it is possible to write (3) using Fourier series with formula (4) and (5). For example, the first equation gives

$$\sum_{k=-H}^{H} \mathrm{e}^{ik\omega t}\left(-k^2\omega^2 x_k + 2\mu ik\omega x_k + x_k + \sum_{\substack{h_1+h_2=k \\ |h_1|\le H, |h_2|\le H}} x_{h_1} y_{h_2}\right) = F\frac{\mathrm{e}^{i\omega t} + \mathrm{e}^{-i\omega t}}{2} \tag{6}$$

Balancing the harmonics yields

$$\begin{aligned} &-k^2\omega^2 x_k + 2\mu i k\omega x_k + x_k + \sum_{\substack{h_1+h_2=k \\ |h_1|\le H, |h_2|\le H}} x_{h_1} y_{h_2} = 0 && \text{if } |k| \neq 1 \\ &-k^2\omega^2 x_k + 2\mu i k\omega x_k + x_k + \sum_{\substack{h_1+h_2=k \\ |h_1|\le H, |h_2|\le H}} x_{h_1} y_{h_2} = \frac{F}{2} && \text{if } |k| = 1 \end{aligned} \tag{7}$$

This is a set of algebraic equations in the unknowns $x_{-H}, x_{-H+1}, \ldots, x_0, x_1, \ldots, x_H$ and possibly ω, μ and F.

2.2 Continuation through asymptotic numerical method

The asymptotic numerical method (ANM) that has first been described in [4–6] relies on a high-order Taylor series representation of the solution branch. This technique has already proven its efficiency for a lot of applications in engineering [10], mechanics [29] or acoustics for example. While some implementations relying on automatic differentiation do exist (see [3] for example) the choice is made here to work with a quadratic framework. A generic implementation of this latest approach which minimizes problem-dependent implementation has been developed [15]. It is based on the numerical continuation of algebraic systems of the form

$$R(V) = 0 \tag{8}$$

where $V \in \mathbb{R}^{n+1}$ and $R(V) \in \mathbb{R}^n$ is an analytic function of its argument. This system is always written in a quadratic format as a prerequisite of the method. Again, this formalism is not a constraint that we suffer but a choice that allows to treat a very wide range of problems as shown in [18]. System (8) can then be written

$$\tilde{R}(\tilde{V}) = C + L(\tilde{V}) + Q(\tilde{V}, \tilde{V}) = 0 \tag{9}$$

where $\tilde{V} \in \mathbb{R}^{N+1}$, $N \geq n$ and C, L and Q are respectively a constant, a linear and a quadratic operator. For small example (3), the introduction of an auxiliary variable $y = x^2$ in the time domain allows to have almost directly a quadratic algebraic system. The only non-quadratic terms are due to derivatives (5) that lead to cubic terms $x_k\omega^2$ or $x_k\mu\omega$ depending on whether ω or/and μ is/are unknown/unknowns as can be seen on algebraic system (7) obtained from HBM. The introduction of the auxiliary variables $\Omega = \omega^2$ and $\Lambda = \mu\omega$ solves this problem.

The coupling between ANM and HBM in quadratic framework (9) can be automatized and is detailed in [8]. Again, the key idea of the ANM is to compute a high-order Taylor series development of the solution branch. Let consider that $\tilde{V}_0$ is a regular solution of system (9). Let $\tilde{V}_1$ be a tangent vector at $\tilde{V}_0$. The classical arc-length parameter $a = \tilde{V}_1^t(\tilde{V}_0 - \tilde{V})$ is introduced, and the solution branch around $\tilde{V} = \tilde{V}_0$ is written as a power series with respect to a

$$\tilde{V}(a) = \tilde{V}_0 + a\tilde{V}_1 + a^2\tilde{V}_2 + a^3\tilde{V}_3 + \cdots \tag{10}$$

Introducing series (10) in Eq. (9) and equating the terms of same power yields :

$$\begin{aligned} &\text{order } 0: \ 0 = C + L(\tilde{V}_0) + Q(\tilde{V}_0, \tilde{V}_0) \\ &\text{order } 1: \ 0 = L(\tilde{V}_1) + Q(\tilde{V}_1, \tilde{V}_0) + Q(\tilde{V}_0, \tilde{V}_1) := J_0(\tilde{V}_1) \\ &\quad \vdots \\ &\text{order } p: \ 0 = J_0(\tilde{V}_p) + \textstyle\sum_{k=1}^{p-1} Q(\tilde{V}_k, \tilde{V}_{p-k}) \\ &\quad \vdots \end{aligned} \tag{11}$$

where J_0 is the Jacobian matrix of the system at the point $\tilde{V}_0$. The order 0 equation states that $\tilde{V}_0$ is a solution of Eq. (9), and the order 1 equation states that $\tilde{V}_1$ is a tangent vector at the solution point $\tilde{V}_0$. Notice that for orders $p \geq 2$, solving linear systems (11) require only one matrix J_0 to be inverted, which is an obvious advantage from a computational cost point of view. More on the implementation of continuation in the case of algebraic systems coming from the harmonic balance method is available in [8]. The next section generalizes this approach for systems with time-delayed variables in their formulation.

3 Continuation of periodic solution of systems with time delay

In this section, a system of delay differential equations, forced or autonomous and possibly neutral, of the following general form is considered:

$$f(t, x(t), \dot{x}(t), x(t-\tau), \dot{x}(t-\tau), \lambda) = 0 \tag{12}$$

where $f : \mathbb{R} \times \left(\mathbb{R}^N\right)^4 \times \mathbb{R} \mapsto \mathbb{R}^N$ is an analytic function that is periodic with respect to its first variable, $x : \mathbb{R} \mapsto \mathbb{R}^N$ is an unknown periodic function of unknown pulsation ω, τ is a real number called the delay and λ is a control parameter of interest called the continuation parameter. The continuation parameter λ may be equal to the delay τ as shown in Sect. 4.1.

A systematic way to recast Eq. (12) quadratically is first to introduce three auxiliary variables :

$$\begin{cases} f(t, x(t), y(t), x_\tau(t), y_\tau(t), \lambda) = 0 \\ y(t) - \dot{x}(t) = 0 \\ x_\tau(t) - x(t-\tau) = 0 \\ y_\tau(t) - y(t-\tau) = 0 \end{cases} \tag{13}$$

The system has now $4N + 1$ unknowns for $4N$ equations. The equations on delayed variables appear isolated, and a classical quadratic recast [8,15,18] can be applied to the function f to write system (13) quadratically :

$$\begin{cases} g(t, x(t), y(t), x_\tau(t), y_\tau(t), \lambda, v(t)) = 0 \\ y(t) - \dot{x}(t) = 0 \\ x_\tau(t) - x(t-\tau) = 0 \\ y_\tau(t) - y(t-\tau) = 0 \end{cases} \tag{14}$$

where $v : \mathbb{R} \mapsto \mathbb{R}^{N_{\text{aux}}}$ is a function of the time that can be expressed as quadratic expressions of all the variables. The system has now $4N+1+N_{\text{aux}}$ unknowns for $4N + N_{\text{aux}}$ quadratic equations. The two last equations are the only one that are not treated in [8,15,18]; thus, the Fourier coefficients of x_τ are now derived from the Fourier coefficients of x with their quadratic recast.

3.1 Harmonic balance method applied to delayed variables

The order of truncation of the Fourier series is noted H. The truncated Fourier series of $t \mapsto x(t)$ is:

$$x(t) = a_0 + \sum_{k=1}^{H} a_k \cos(k\omega t) + b_k \sin(k\omega t) \tag{15}$$

The Fourier series of $t \mapsto x(t-\tau)$ is:

$$\begin{aligned} x(t-\tau) =& a_0 + \sum_{k=1}^{H} a_k \cos(k\omega(t-\tau)) \\ &+ \sum_{k=1}^{H} b_k \sin(k\omega(t-\tau)) \\ =& a_0 + \sum_{k=1}^{H} a_k[\cos(k\omega t)\cos(k\omega\tau) \\ &+ \sin(k\omega t)\sin(k\omega\tau)] \\ &+ \sum_{k=1}^{H} b_k[\sin(k\omega t)\cos(k\omega\tau) \\ &- \cos(k\omega t)\sin(k\omega\tau)] \\ =& a_0 + \sum_{k=1}^{H} [a_k \cos(k\omega\tau) \\ &- b_k \sin(k\omega\tau)]\cos(k\omega t) \\ &+ \sum_{k=1}^{H} [b_k \cos(k\omega\tau) \\ &+ a_k \sin(k\omega\tau)]\sin(k\omega t) \end{aligned} \tag{16}$$

Therefore, if a_k^τ and b_k^τ are the Fourier coefficients of $t \mapsto x(t-\tau)$, their expression is given by:

$$\begin{aligned} a_0^\tau &= a_0 \\ a_k^\tau &= a_k \cos(k\omega\tau) - b_k \sin(k\omega\tau)\,, \quad k \geq 1 \\ b_k^\tau &= b_k \cos(k\omega\tau) + a_k \sin(k\omega\tau)\,, \quad k \geq 1 \end{aligned} \tag{17}$$

3.2 Asymptotic numerical method applied to delayed variables

For $k \geq 1$, the auxiliary variables $c_k^\tau = \cos(k\omega\tau)$ and $s_k^\tau = \sin(k\omega\tau)$ are defined to get a quadratic recast for (17):

$$\begin{aligned} \tilde{\tau} &= \omega\tau \\ a_0^\tau &= a_0 \\ a_k^\tau &= a_k c_k^\tau - b_k s_k^\tau \\ b_k^\tau &= b_k c_k^\tau + a_k s_k^\tau \\ s_k^\tau &= \sin(k\tilde{\tau}) \quad \text{and} \quad \mathrm{d}(s_k^\tau) = k c_k^\tau \times \mathrm{d}(\tilde{\tau}) \\ c_k^\tau &= \cos(k\tilde{\tau}) \quad \text{and} \quad \mathrm{d}(c_k^\tau) = -k s_k^\tau \times \mathrm{d}(\tilde{\tau}) \end{aligned} \tag{18}$$

where in the last two equations, the differentiated forms are used as explained in [15] to compute the Taylor series expansions (10) of s_k^τ and c_k^τ. The last equations are defined as "initial conditions" plus a "differential system". For the computation of Taylor series (10), the "initial conditions" are used to compute the zeroth-order coefficient $\tilde{V}_0$ and the differential system to compute higher-order coefficients $\tilde{V}_p$, $p \geq 1$. This type of computation of Taylor series development is explained in detail in the book [14]. The main ideas are recalled below.

Let $x = x_0 + ax_1 + a^2x_2 + \cdots$ be a given Taylor series and let $s = \sin(x)$ and $c = \cos(x)$ be its sine and its cosine. To compute the coefficients of the Taylor

series of s $(= s_0 + as_1 + a^2 s_2 + \cdots)$ and c $(= c_0 + ac_1 + a^2 c_2 + \cdots)$, the following procedure is applied:

- $s_0 = \sin(x_0)$ and $c_0 = \cos(x_0)$.
- For $p \geq 1$, identify the term of order $p-1$ in the differentiated equations $\mathrm{d}s = c\mathrm{d}x$ and $\mathrm{d}c = -s\mathrm{d}x$.

For the second step, the development in Taylor series of the differentiated equations is written:

$$\begin{aligned} s_1 + 2as_2 + 3a^2 s_3 + \cdots &= \left(c_0 + ac_1 + a^2 c_2 + \cdots\right) \\ &\quad \left(x_1 + 2ax_2 + 3a^2 x_3 + \cdots\right) \\ c_1 + 2ac_2 + 3a^2 c_3 + \cdots &= -\left(s_0 + as_1 + a^2 s_2 + \cdots\right) \\ &\quad \left(x_1 + 2ax_2 + 3a^2 x_3 + \cdots\right) \end{aligned} \tag{19}$$

For $p = 1$, the identification of the constant term of system (19) gives $s_1 = c_0 x_1$ and $c_1 = -s_0 x_1$. For $p \geq 1$, the identification of the terms of order $p-1$ in system (19) gives the following recursive formula:

$$\begin{aligned} s_p &= \frac{1}{p}\left[c_0 \times p x_p + c_1 \times (p-1)x_{p-1} + \cdots \right. \\ &\quad \left. + c_{p-2} \times 2x_2 + c_{p-1} \times x_1\right] \\ c_p &= -\frac{1}{p}\left[s_0 \times p x_p + s_1 \times (p-1)x_{p-1} + \cdots \right. \\ &\quad \left. + s_{p-2} \times 2x_2 + s_{p-1} \times x_1\right] \end{aligned} \tag{20}$$

4 Applications

In this section, four examples are given which have been explored with our method. The first one, a delay Van der Pol oscillator [1], is autonomous. It is used to show the convergence of the Fourier series to a reference solution of the system, computed with a standard solver [25]. Moreover, a bifurcation diagram with respect to the delay is drawn and the location of the many Hopf bifurcations is ascertained with the results of a linear stability analysis. The second example, a forced delay Duffing oscillator [17], exhibits a lot of resonances (both superharmonic and subharmonic). Its bifurcation diagram is represented with a focus on two symmetry-breaking bifurcations. The third example is a toy model of clarinet [26] that is purely algebraic. Its periodic solutions are squared shaped, and their Fourier series converge rather slowly. This example shows the robustness of our approach. The fourth and last example is a neutral model of saxophone [9,19] using transcendental functions in its writing. A solution is compared to a finite-difference scheme from the literature [19] and a bifurcation diagram is drawn, showing an expected behaviour for this type of system according to [11].

4.1 A delay Van der Pol oscillator

In this part, we consider the Van der Pol oscillator (dimensionless) with delay feedback that has been studied in [1]:

$$\ddot{u}(t) - \varepsilon(1 - u(t)^2)\dot{u}(t) + u(t) = \varepsilon k u(t-\tau) \tag{21}$$

The continuation is performed with respect to τ. Introducing the auxiliary variables $v(t) = \dot{u}(t)$, $r(t) = 1 - u(t)^2$ and $\mathrm{F_{nl}}(t) = v(t)r(t) - ku(t-\tau)$. In order to minimize the number of auxiliary variables, the variable $\mathrm{F_{nl}}$ is the sum of the delayed variable $ku(t-\tau)$ (with k constant) and the product $v \times r$. Hence the delayed variable is not isolated like in (13) and (14), but as it appears linearly, this allows to use the approach explained in the previous section. The following quadratic recast is used:

$$\begin{aligned} \dot{v}(t) + u(t) - \varepsilon \mathrm{F_{nl}}(t) &= 0 \\ v(t) - \dot{u}(t) &= 0 \\ r(t) - 1 + u(t)^2 &= 0 \\ \mathrm{F_{nl}}(t) - v(t)r(t) - ku(t-\tau) &= 0 \end{aligned} \tag{22}$$

To validate the method, Fig. 1 shows the difference between time integration and harmonic balance for the periodic solution of Eq. (21) obtained with $\varepsilon = 2$, $\tau = 0.2$ and $k = 0.2$. The number of harmonics is varied to show the convergence of the harmonic balance towards the time integration solution. The reference solution is a time integration performed with *dde23* built-in solver of MATLAB. Its absolute and relative tolerance thresholds have been set to 10^{-8}.

With a low number of harmonics, i.e. for $H < 10$, the solution is not accurate and even the period of the oscillation is not computed correctly. Indeed, the plot $H = 5$ stops before $t = 10\,\mathrm{s}$, conversely to the other plots. From $H = 25$ to $H = 50$, the solution gets much closer to the reference. Solutions for $H = 100$ and $H = 200$ look superimposed. In fact, the tolerance at which the reference has been computed, i.e. 10^{-8}, is reached for $H = 50$. When computing the solution with a higher number of harmonics, the time-integration reference is probably farther from the true

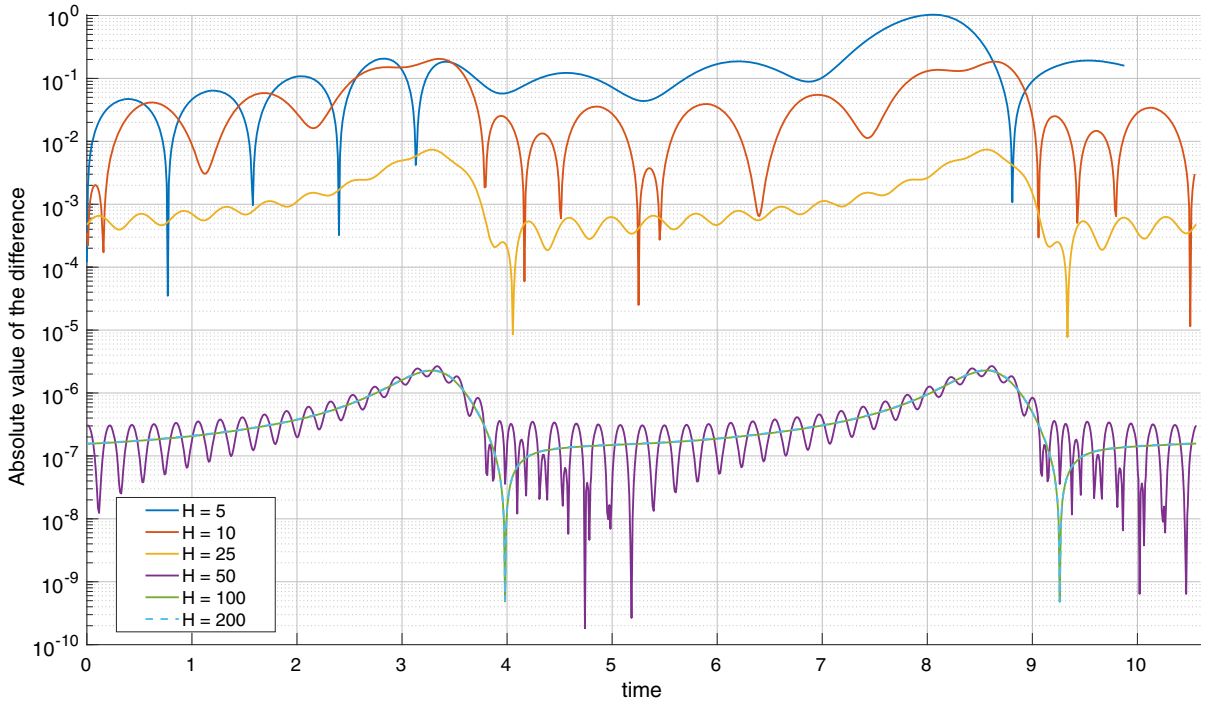

Fig. 1 Differences over one period between several solutions of Eq. (21) obtained with the harmonic balance method with increasing H and a reference solution obtained with time integration. Here $\varepsilon = 2$, $\tau = 0.2$ and $k = 0.2$

solution than the solution obtained with the harmonic balance method. In addition, the time-integration solver used takes approximately ten times the time needed to compute the solution with $H = 50$. Moreover, once a solution has been computed the computation of the bifurcation diagram through ANM is very fast : for the same computation time as one time integration over twenty periods (to get rid of the transient), all the steady state solutions between $\varepsilon = 2$ and $\varepsilon = 5$ are available with our method.

Figure 2 shows a part of the bifurcation diagram of system (21) with the delay τ as a continuation parameter. There are infinitely many Hopf bifurcations in this system. The analytic position of the Hopf bifurcations is determined by the stability analysis of the equilibrium $u = 0$ and is given by the solutions of the system [1]:

$$\begin{cases} 1 - \omega^2 = k\varepsilon \cos(\tau\omega) \\ \varepsilon\omega \quad\quad = k\varepsilon \sin(\tau\omega) \end{cases} \tag{23}$$

where ω is the pulsation of the arising periodic solution at the corresponding Hopf point. The continuation of the periodic solution branches has been initialized with an analytic approximation with $H = 1$ and the pulsation ω solution of system (23) for the corresponding value of τ. In this particular case, the robustness of the ANM allows to follow all the solution branches from just one starting point. In the general case, it would probably necessitate to initialize with an analytic approximation at every Hopf bifurcations. On Fig. 2, some parts of the diagram are of null amplitude : these are just some parts where the solution found is the equilibrium $u = 0$.

4.2 A forced delay Duffing oscillator

The example presented in this section is taken from [17]. It is an example of a forced delay differential equation. The dimensionless equation of motion (Eq. (3) in the reference) is :

$$\begin{aligned} &\ddot{x}(t) + 2\zeta\dot{x}(t) + x(t) + \mu x^3(t) \\ &\quad = 2ux(t-\tau) + 2v\dot{x}(t-\tau) + f\cos(\lambda t) \end{aligned} \tag{24}$$

The continuation is performed with respect to λ. The following quadratic recast is used :

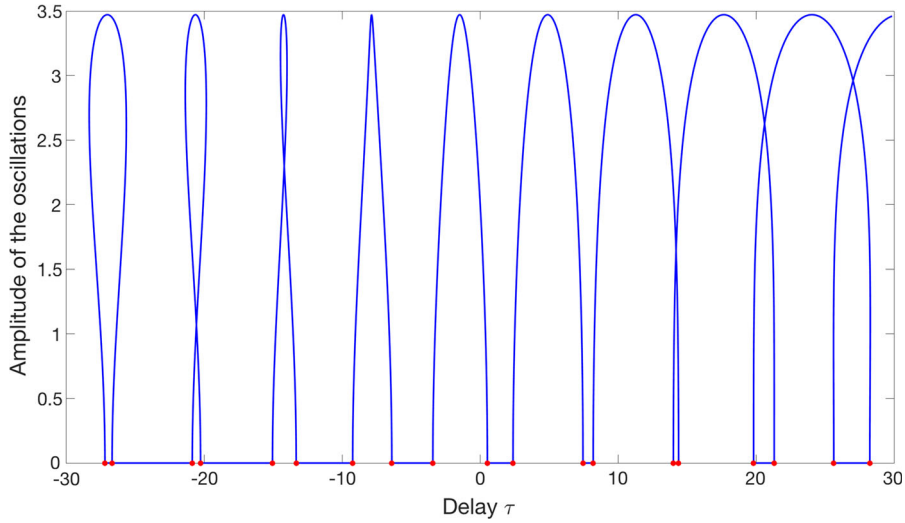

Fig. 2 Bifurcation diagram of Eq. (21) with respect to the delay τ, $\varepsilon = 0.1$ and $k = 2$. There are as many Hopf bifurcations as branches starting from a null amplitude. The red dots are the analytical position of Hopf bifurcations given by the solutions of system (23). (Color figure online)

$$\begin{aligned}
&\dot{x}(t) - y(t) = 0\\
&\dot{y}(t) + 2\zeta y(t) + x(t) + \mu r(t)x(t)\\
&\quad - 2ux(t-\tau) - 2vy(t-\tau) = f\cos(\lambda t)\\
&r(t) - u(t)^2 = 0
\end{aligned} \tag{25}$$

where λ is the continuation parameter and the set of parameters used is : $\zeta = \varepsilon$, $\mu = \varepsilon$, $u = \varepsilon$, $v = -\varepsilon$, $\tau = \pi$ and $f = 5$ with $\varepsilon = 0.05$. Again, the time-delayed terms are not isolated but as they appear linearly in the equations, the recast of Sect. 3 is applicable. In [17], the primary and the 1/3 subharmonic resonances were studied with the method of multiple scales. In this present article a whole bifurcation diagram is drawn, showing both primary and 1/3 subharmonic resonances. To find the starting point of the continuation, the approximations computed in [17] are used. The forcing amplitude has been chosen high to have a rich dynamics as can be seen in the bifurcation diagram which is represented in Fig. 3. To draw this diagram, the order of truncation of the Fourier series has been set to $H = 25$ which is sufficient away from superharmonic resonances. The 1/3 subharmonic resonance is disconnected from the main branch. It corresponds to a solution branch where the pulsation of the oscillation verifies $\omega = \frac{\lambda}{3}$.

The zoom on the top of Fig. 3 shows the many superharmonic resonances and the symmetry-breaking (SB) bifurcations. The superharmonic resonances appear for $\lambda \gtrsim \frac{1}{2p+1}$, $p \in \mathbb{N}$ and in these areas the solutions become more complex as the harmonics $2p+1$ are close to the natural pulsation of the system. In addition, two symmetry-breaking bifurcations are detected and the emerging solution is then continued with the method explained in [7]. On the bifurcated branches, the solutions have strong even harmonics appearing and their phase diagrams $(x, \dot{x})$ are no longer symmetric.

4.3 A clarinet toy model

The following example is a simplified model of clarinet-like instrument, taken from [26] [Eqs. (4)-(5)-(6)-(7)-(10)]. This system has been chosen to highlight that our approach copes even with a degenerate form of general system (12). In this example, there are no time derivatives in the equations of the motion. The unknowns are functions of the time and the dynamics comes from the coupling between a nonlinearity and an equation with time-delayed variable. As in the reference, the reed dynamics is neglected and the dimensionless equations can be written :

$$\begin{aligned}
u(t) &= \begin{cases} 0 & \text{if } p(t) \le \gamma - 1 \\ \zeta(p(t) - \gamma + 1)\sqrt{|\gamma - p(t)|}\,\mathrm{sign}(\gamma - p(t)) & \text{if } p(t) > \gamma - 1 \end{cases}\\
p^-(t) &= -\lambda p^+(t - \tfrac{2\ell}{c})
\end{aligned} \tag{26}$$

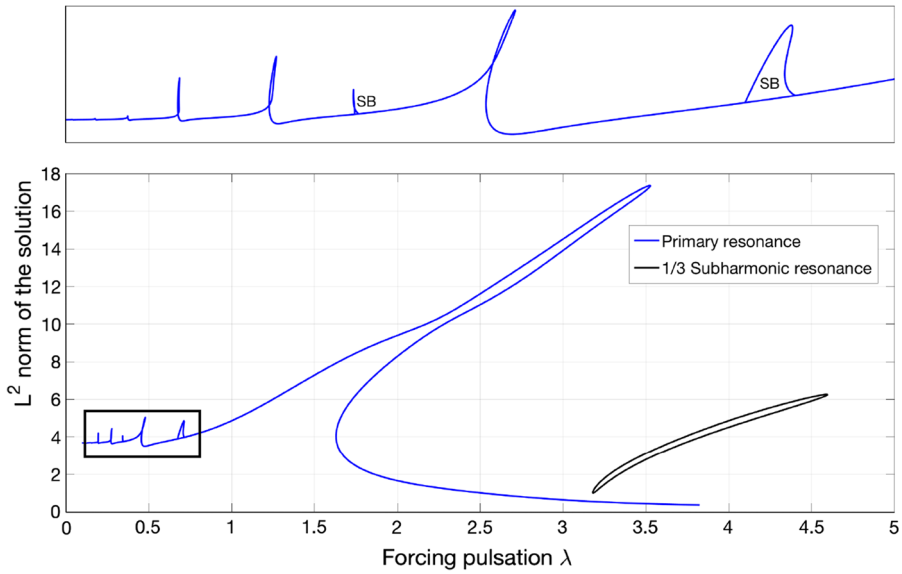

Fig. 3 Bifurcation diagram of the amplitude of the solution with respect to the forcing pulsation λ. On the primary resonance solution branch, there are several superharmonic resonances appearing for $\lambda = \frac{1}{3}, \frac{1}{5}, \frac{1}{7}, \frac{1}{9}, \ldots$. There are also two symmetry-breaking bifurcation, noted SB on the zoom of the diagram, detected with the method explained in [7] for which even harmonics appear

where p and u are respectively the acoustic pressure and the volume flow in the mouthpiece of the instrument. p^+ and p^- are respectively the forward and the backward progressive waves, linked to p and u through $p = p^- + p^+$ and $u = p^+ - p^-$. ℓ is the length of the instrument and c is the speed of sound. The delay $\frac{2\ell}{c}$ in Eq. (26) represents the time for a pressure wave to go back and forth the cylindrical bore of the clarinet. λ is the reflection coefficient at the end of the instrument which can be seen as a damping term. γ is the static blowing pressure in the mouth of the player and ζ is the reed parameter. All the variables but the time are dimensionless in this model. In the following, the time is normalized by $\frac{2\ell}{c}$ so that the value of the delay τ is 1. For simplicity, the nonlinear characteristics (the first equation of system (26)) is written under the assumption that $-1 < p - \gamma < 0$ which means according to [26] that the reed channel is open and air is allowed to enter the clarinet. System (26) becomes

$$\begin{aligned} u(t) &= \zeta(p(t) - \gamma + 1)\sqrt{\gamma - p(t)} \\ p^-(t) &= -\lambda p^+(t-1) \end{aligned} \tag{27}$$

Its quadratic recast is

$$\begin{aligned} p^-(t) &= -\lambda p^+(t-1) \\ v(t)^2 &= \gamma - p(t) \\ u(t) &= \zeta(p(t) - \gamma + 1)v(t) \end{aligned} \tag{28}$$

The variable $v(t)$ is defined implicitly by the second equation. To ensure that the results are correct, we have to check that $v(t)$ is non-negative. The parameters chosen are $\lambda = 0.95$ and $\zeta = 0.8$. The continuation is performed with respect to γ, the dimensionless blowing pressure. The bifurcation diagram is plotted in Fig. 4.

The values for which the system encounters a Hopf bifurcation $\gamma_H = 0.35$ or a period doubling bifurcation $\gamma_{\mathrm{PD}} = 0.43$ are the same as the one given in [26] (table 1) up to the third significant digit. On Fig. 4, the Hopf bifurcation occurs at the lowest point of the solution branch. As the mean value of p is not zero, the L^2 norm of p is not 0 at the bifurcation point. The exact solution of this system in the time domain is a square, and the decomposition in Fourier series is obviously not very well suited for this discontinuous type of signal. However, the numerical method is so robust that it is able to continue this solution on the whole domain which is remarkable. This also explains why the diagram represents the L^2 norm of p and not its amplitude : Gibbs phenomenon leads to an overshoot at each of the two discontinuous point of the signal. This gives wrong amplitude for the acoustic pressure. The analytical solutions given in [26] were used as starting points for the continuation process, using their truncated decomposition in Fourier series.

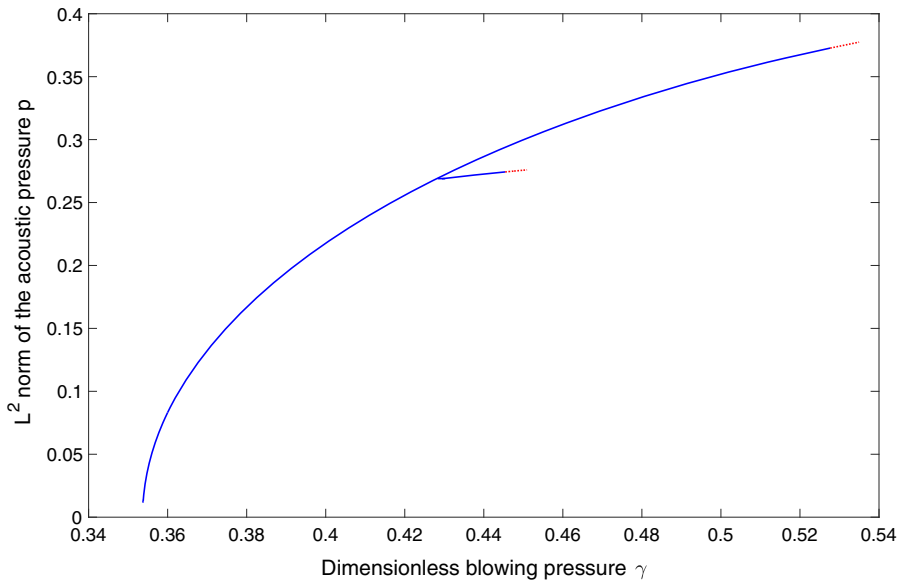

Fig. 4 Bifurcation diagram of the toy model of clarinet (27) with respect to the dimensionless blowing pressure γ, with $H = 200$. The period doubling bifurcation is visible as the connection of the branches. The red dotted lines correspond to section of branches where the variable $v(t)$ is negative, i.e. where the simplified model is not valid anymore to represent the clarinet functioning. (Color figure online)

4.4 A neutral saxophone model

In this section, a neutral system that is a dimensionless model of saxophone taken from [19] is studied. It has also been the subject of the conference talk [9]. The derivative of Eq. (40) in [19] is taken to get rid of the integrals. This will be taken into account when considering the Fourier developments of the unknowns. The following equation is obtained :

$$\begin{aligned}&\ddot{p} + \sqrt{3}(1 - F'(p))\dot{p} + p \\ &\quad = \ddot{p}_\tau + \sqrt{3}(-1 - F'(p_\tau))\dot{p}_\tau + p_\tau \end{aligned} \tag{29}$$

where p is the acoustic pressure in the mouthpiece of the instrument; γ and ζ have the same meaning as in Sect. 4.3. Everytime there is a τ index, it means that the variable is delayed, i.e. $p_\tau(t) = p(t - \tau)$. In order to have a smooth function, the nonlinear characteristics $F(p)$ is an exponential regularized law [9] :

$$F(p) = \zeta \frac{e}{\sqrt{3}} e^{3(p-\gamma)}(3(p - \gamma))(\gamma - p) \tag{30}$$

To recast Eq. (29) quadratically, the idea is to write it on the form $I + \sqrt{3}\dot{p} = I_\tau - \sqrt{3}\dot{p}_\tau$ with $I = \ddot{p} - \sqrt{3}F'(p)\dot{p} + p$. It is then necessary to write $F'(p)$ quadratically. This is done using the same idea as for the recast in Eq. (18) ; setting $\Delta p = p - \gamma$, the exponential is written using $A = e^{3(p-\gamma)}(3\Delta p)$ and its differentiated form $\mathrm{d}A = 3A\mathrm{d}(\Delta p)$. These remarks lead to introduce the following auxiliary variables :

$$\begin{aligned} \Delta p &= p - \gamma \\ A &= e^{3(p-\gamma)}(3\Delta p) \\ F'(p) &= \zeta \frac{e}{\sqrt{3}} A(-1 - 3\Delta p) \\ q &= \dot{p} \\ I &= \ddot{p} + p - \sqrt{3}F'(p)q \end{aligned} \tag{31}$$

which allows to write Eq. (29) in a quadratic format:

$$\begin{aligned} I - I_\tau + \sqrt{3}(q + q_\tau) &= 0 \\ \Delta p - (p - \gamma) &= 0 \\ A - e^{3(p-\gamma)}(3\Delta p) &= 0 \text{ and } \mathrm{d}A - 3A\,\mathrm{d}(\Delta p) = 0 \\ F'(p) - \zeta \frac{e}{\sqrt{3}} A(-1 - 3\Delta p) &= 0 \\ q - \dot{p} &= 0 \\ I - (\ddot{p} + p - \sqrt{3}F'(p)q) &= 0 \end{aligned} \tag{32}$$

The definition of A (third line, left-hand side in (32)) is used only to compute the mean value (or the constant term) of its Fourier series and its differentiated form (third line, right-hand side in (32)) is used to compute higher-order terms. This has been explained in [18]. The dimensionless delay τ can be expressed in terms of the length of the conical resonator ℓ of the saxophone, truncated at its input to plug the mouthpiece, and the length x_1 of the missing part of the cone (from the apex to the input of the truncated cone). This is not our purpose here to understand the refinements of this model, the interested reader can find the details in [19].

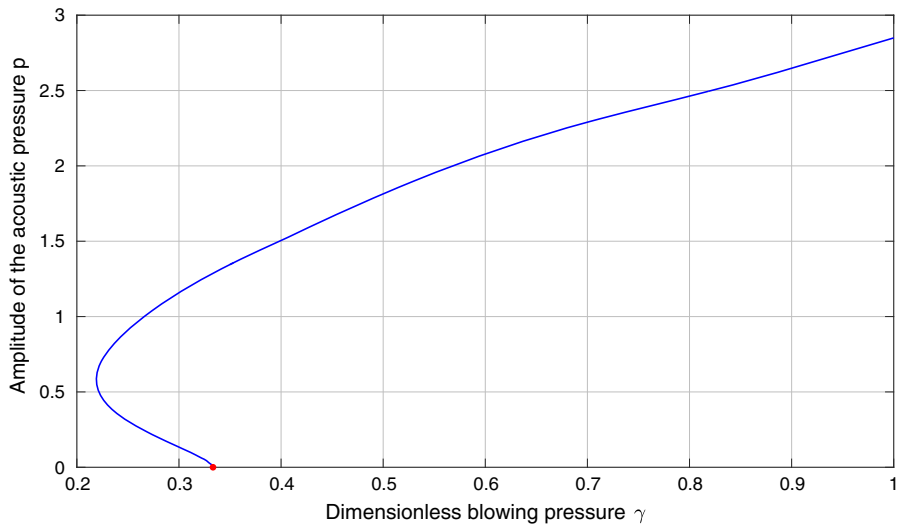

Fig. 5 Bifurcation diagram of a model of saxophone with respect to the dimensionless blowing pressure γ and for $\zeta = 1.2$. The subcritical Hopf bifurcations can be seen clearly. It is not surprising for the saxophone to show such subcritical bifurcations [11]. This diagram has been computed using $H = 50$ harmonics

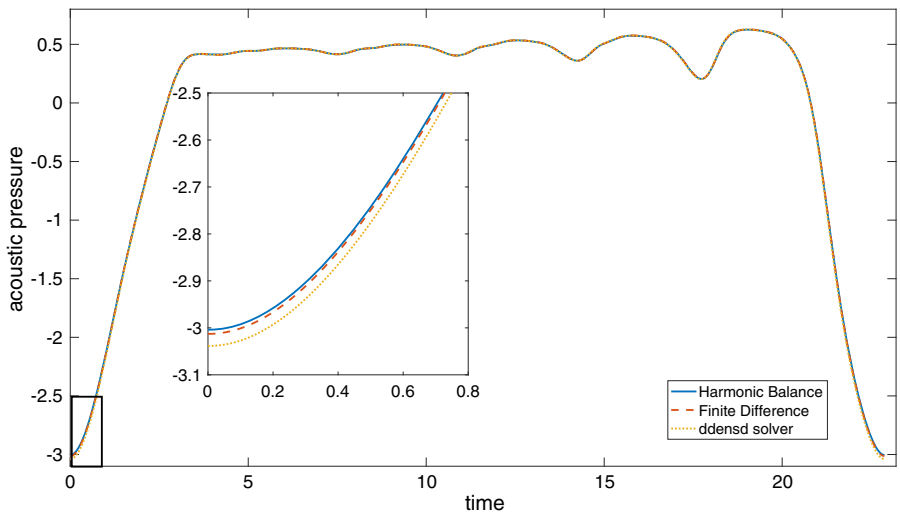

Fig. 6 Comparison of the periodic solutions of Eq. (29) over one period for $\zeta = 1.2$ and $\gamma = 0.5$. In blue, the solution obtained with harmonic balance method with $H = 50$ and extracted from the bifurcation diagram shown in Fig. 5. In red dashed, the solution obtained with the time-integration algorithm of [19] with 5000 samples per period. In yellow dotted, the solution obtained with *ddensd* Matlab's solver with absolute and relative thresholds set to 10^{-3}. A zoom on the zone of beating reed is shown to enhance the differences between the waveforms. (Color figure online)

Below, the value of τ is set to $\frac{2\sqrt{3}\ell}{x_1}$ with $\ell = \frac{17}{15}$ and $x_1 = \frac{1}{5}$. ζ is set to 1.2 to draw the bifurcation diagram with respect to γ in Fig. 5. As said above, Eq. (29) is the derivative of another equation. This implies that after the harmonic balance method (HBM) has been performed, the constant coefficient equation (i.e. its mean value) states $0 = 0$. As this leads to a singular system, this equation is replaced by $p^0 = 0$ where p^0 is the constant term [the a_0 of Fourier decomposition (15)] of p.

The waveform of each unknown over one period is a by-product of the method and is available for each value of γ, i.e. for each point of bifurcation diagram 5. The waveform of p is compared to the one obtained with the numerical integration algorithm presented in [19] for $\gamma = 0.5$ and is in very good agreement as can be seen in Fig. 6. On the same figure, the pressure obtained by integration with the built-in solver *ddensd* [24] of MATLAB is presented. The three methods give very close results. However, as expected in [19], their scheme is

unstable and the Hopf bifurcation is detected around $\gamma = 0.285$, that is, below the theoretical value of $\gamma = \frac{1}{3}$ which is found with our method.

The scheme used in [19] is very fast but requires a high sampling frequency (more than 1000 samples per period) to converge. The *ddensd* solver takes a longer time especially when the tolerance chosen is decreased to the minimum value possible of 10^{-5}. In our approach, the transient is not available but the shape of the steady state is obtained on all the solution branch instantly through the Fourier series construction, as well as the unstable periodic regimes. In addition, the Hopf bifurcation and the limit point can be deduced from the bifurcation diagram.

The model of saxophone presented should have a zero mean over one period by physical consideration [19]. For the signals represented in Fig. 6, the acoustic pressure obtained by Harmonic Balance has a mean value around the numerical precision 10^{-16} while the time integration solver from [19] gives a mean around 10^{-4} and *ddensd* gives 10^{-3}.

5 Conclusion

An extension of the HBM, coupled with the ANM continuation, to time-delay systems is developed. Various types of systems exhibiting constant time delays is explored. Especially, delay differential equations of neutral type do not require a specific setting in the framework presented. The available tools of the ANM continuation allow to compute bifurcated branches without the need of a specific implementation.

The coupling between HBM and ANM shows its efficiency and its robustness compared to time-integration methods. Especially in some cases where there are not many numerical methods available (neutral systems) and even when the Fourier series of the periodic solution have bad convergence properties. It is ascertained by a comparison to time-domain solvers. The algorithms used for this article are freely available online at http://manlab.cnrs-mrs.fr.

The main perspective of this work would be to implement a robust frequency-based method for the stability analysis of delay differential equations. For equilibrium as well as for periodic solution, this would allow full bifurcation analysis of delay systems.

Acknowledgements The authors want to thank Tom Colinot for the help with the saxophone model and its associated time-integration method. This work has been carried out in the framework of the Labex MEC (ANR-10-LABX-0092) and of the A*MIDEX project (ANR-11-IDEX-0001-02), funded by the Investissements d'Avenir French Government program managed by the French National Research Agency (ANR). Conflict of Interest: The authors declare that they have no conflict of interest.

References

1. Atay, F.M.: Van der Pol's oscillator under delayed feedback. J. Sound Vib. **218**(2), 333–339 (1998)
2. Barton, D.A., Krauskopf, B., Wilson, R.E.: Collocation schemes for periodic solutions of neutral delay differential equations. J. Differ. Equ. Appl. **12**(11), 1087–1101 (2006)
3. Charpentier, I., Cochelin, B.: Towards a full higher order AD-based continuation and bifurcation framework. Optim. Methods Softw. **33**, 945–962 (2018)
4. Cochelin, B.: A path-following technique via an asymptotic-numerical method. Comput. Struct. **53**(5), 1181–1192 (1994)
5. Cochelin, B., Damil, N., Potier-Ferry, M.: Asymptotic-numerical methods and pade approximants for non-linear elastic structures. Int. J. Numer. Methods Eng. **37**(7), 1187–1213 (1994)
6. Cochelin, B., Damil, N., Potier-Ferry, M.: The asymptotic-numerical method: an efficient perturbation technique for nonlinear structural mechanics. Revue européenne des éléments finis **3**(2), 281–297 (1994)
7. Cochelin, B., Medale, M.: Power series analysis as a major breakthrough to improve the efficiency of asymptotic numerical method in the vicinity of bifurcations. J. Comput. Phys. **236**, 594–607 (2013)
8. Cochelin, B., Vergez, C.: A high order purely frequency-based harmonic balance formulation for continuation of periodic solutions. J. Sound Vib. **324**(1), 243–262 (2009)
9. Colinot, T., Kergomard, J.: Formulation analytique de la pression interne d'un modèle idéalisé d'instrument conique à anche. In: CFA 2018/VISHNO (2018)
10. Cottanceau, E., Thomas, O., Véron, P., Alochet, M., Deligny, R.: A finite element/quaternion/asymptotic numerical method for the 3D simulation of flexible cables. Finite Elem. Anal. Des. **139**, 14–34 (2018)
11. Dalmont, J.P., Gilbert, J., Kergomard, J.: Reed instruments, from small to large amplitude periodic oscillations and the Helmholtz motion analogy. Acta Acust. United Acust. **86**(4), 671–684 (2000)
12. Engelborghs, K., Luzyanina, T., Roose, D.: Numerical bifurcation analysis of delay differential equations using DDE-BIFTOOL. ACM Trans. Math. Softw. (TOMS) **28**(1), 1–21 (2002)
13. Fourier, J.: Theorie analytique de la chaleur, par M. Fourier. Chez Firmin Didot, père et fils (1822)
14. Griewank, A., Walther, A.: Evaluating Derivatives: Principles and Techniques of Algorithmic Differentiation, vol. 105. SIAM, Philadelphia (2008)
15. Guillot, L., Cochelin, B., Vergez, C.: A generic and efficient taylor series based continuation method using a quadratic

recast of smooth nonlinear systems. Int. J. Numer. Methods Eng. (2019). https://doi.org/10.1002/nme.6049
16. Guillot, L., Vigué, P., Vergez, C., Cochelin, B.: Continuation of quasi-periodic solutions with two-frequency harmonic balance method. J. Sound Vib. **394**, 434–450 (2017)
17. Hu, H., Dowell, E.H., Virgin, L.N.: Resonances of a harmonically forced duffing oscillator with time delay state feedback. Nonlinear Dyn. **15**(4), 311–327 (1998)
18. Karkar, S., Cochelin, B., Vergez, C.: A high-order, purely frequency based harmonic balance formulation for continuation of periodic solutions: the case of non-polynomial nonlinearities. J. Sound Vib. **332**(4), 968–977 (2013)
19. Kergomard, J., Guillemain, P., Silva, F., Karkar, S.: Idealized digital models for conical reed instruments, with focus on the internal pressure waveform. J. Acoust. Soc. Am. **139**(2), 927–937 (2016)
20. Krylov, N.M., Bogoliubov, N.N.: Introduction to Non-linear Mechanics. Princeton University Press, Princeton (1949)
21. Liu, L., Kalmár-Nagy, T.: High-dimensional harmonic balance analysis for second-order delay-differential equations. J. Vib. Control **16**(7–8), 1189–1208 (2010)
22. Nakhla, M., Vlach, J.: A piecewise harmonic balance technique for determination of periodic response of nonlinear systems. IEEE Trans. Circuits Syst. **23**(2), 85–91 (1976)
23. Seydel, R.: From Equilibrium to Chaos: Practical Bifurcation and Stability Analysis. North-Holland, Amsterdam (1988)
24. Shampine, L.F.: Dissipative approximations to neutral DDEs. Appl. Math. Comput. **203**(2), 641–648 (2008)
25. Shampine, L.F., Thompson, S.: Solving DDEs in Matlab. Appl. Numer. Math. **37**(4), 441–458 (2001)
26. Taillard, P.A., Kergomard, J., Laloë, F.: Iterated maps for clarinet-like systems. Nonlinear Dyn. **62**(1–2), 253–271 (2010)
27. Vigué, P., Vergez, C., Karkar, S., Cochelin, B.: Regularized friction and continuation: comparison with Coulomb's law. J. Sound Vib. **389**, 350–363 (2017)
28. Vigué, P., Vergez, C., Lombard, B., Cochelin, B.: Continuation of periodic solutions for systems with fractional derivatives. Nonlinear Dyn. **95**, 1–15 (2018)
29. Zahrouni, H., Cochelin, B., Potier-Ferry, M.: Computing finite rotations of shells by an asymptotic-numerical method. Comput. Methods Appl. Mech. Eng. **175**(1–2), 71–85 (1999)
30. Zahrouni, H., Potier-Ferry, M., Elasmar, H., Damil, N.: Asymptotic numerical method for nonlinear constitutive laws. Revue européenne des éléments finis **7**(7), 841–869 (1998)